

용융(60 몰% AlCl_3 -40 몰% NaCl)염 속에서의 알루미늄전극의 반응속도론적 연구

G. F. Uhlig · T. N. Andersen · S. Johns · H. Eyring

미국 유타대학교 화학과

(1974. 7. 12 접수)

A Kinetic Study of the Aluminum Electrode in Molten 60 Mole Percent AlCl_3 -40 Mole Percent NaCl at 453° K

G. F. Uhlig, T. N. Andersen, S. Johns, and H. Eyring

Department of Chemistry, University of Utah, Salt Lake City,

Utah 84112, U. S. A.

(Received July 12, 1974)

요 약. 60 몰% AlCl_3 -40 몰% NaCl 의 용융염(453°K)속에서 알루미늄 전극에 대하여 전류-전압 편극곡선을 얻었다. 50 mA/cm²보다 큰 전류밀도에서는 음-저항에 의한 전위차가 양극전위에 상당히 기여하므로 저항이 큰 AlCl_3 (혹은 AlCl_3 의 농도가 큰 멜트)의 층이 양극표면에 가까이 형성된다고 결론지었다. IR-전위차에 대하여 보정한 후의 Tafel 곡선과 Allen-Hickling 곡선으로 부터 전이 계수, $\alpha_a = (2.3 RT/F)(d \log i/d\eta) = 1.5 \pm 0.25$ 가 얻어졌다. 약 30 mA/cm²보다 큰 음극전류밀도에서는 느린 이온확산과 dendrite 성장 때문에 속도론적 측정이 방해 받았다.

Abstract. Steady-state anodic and cathodic polarization curves were developed for the Al electrode in 60 mole % AlCl_3 -40 mole % NaCl at 180°C(453°K). Ohmic resistance contributed substantially to the anodic polarization at current densities greater than 50 mA/cm² even with capillary tip placed close to the electrode. This could not be rationalized from the resistivity of the melt, which would lead to a much smaller polarization. It was therefore concluded that a layer of high resistance AlCl_3 (or AlCl_3 -rich melt) formed close to the anode surface. From the IR-corrected anodic Tafel and Allen-Hickling plots an apparent anodic charge-transfer coefficient of $\alpha_a = (2.3 RT/F)(d \log i/d\eta) = 1.5 \pm 0.25$ was obtained. At cathodic current densities greater than approximately 30 mA/cm², slow ion diffusion and dendrite growth both interfered with the measurement of the kinetic parameters.

Introduction

The aluminum electrode in molten halide electrolytes has received attention as a candidate anode in rechargeable batteries because of its low equivalent weight, relatively low cost and

negative potential. The kinetics of this system, which are important to the operation and the engineering of a battery, have not previously been established. From steady-state and transient polarization studies of Al in $\text{NaCl}/\text{AlCl}_3$ melts Piontelli, *et al.*¹ and King, *et al.*² concluded

that nearly all the measured potential change, when current is passed, is due to the resistance of the electrolyte. Brabson and coworkers³ constructed Al/Cl₂ cells in which essentially all of the potential drop was determined to be ohmic at anodic current densities up to 600 mA/cm². No electrode kinetics were determined from any of these studies.

Del Duca⁴ concluded that the solution resistance accounted for less than 5 percent of the electrode polarization in her tests of Al in AlCl₃-NaCl and AlCl₃-(LiCl-KCl)_{eut} melts. After correcting steady-state polarization data for the (IR) drop in solution, the above author determined that charge-transfer is rate-controlling at high overvoltages and that surface diffusion of aluminum adions is rate-determining at overvoltages, η , of less than 80 to 150 mV, depending on the system and direction of polarization. From polarization measurements at times <15 μ s (so as to eliminate concentration effects) Schulze and Hoff⁵ determined charge-transfer kinetics at overpotentials less than 50 mV. The IR drop in the AlCl₃-alkali metal melt was compensated for in the measurement circuit and thereby eliminated. These investigators⁵ obtained transfer coefficients and exchange current

densities very different from those of Del Duca⁴, as shown in Table 1; accordingly the rate-determining step was interpreted differently in the two cases. The large differences in the kinetics noted between the results of the above two investigators cannot be reasonably explained in terms of difference in melt compositions; each investigator studied several different electrolytes (cf. Table 1) which yielded kinetic differences much smaller than those between the two studies. Likewise temperature differences as small as those noted in Table 1 have been shown^{4,5} to have no influence on the transfer coefficients and no significant influence on the exchange current densities.

From the non-overlap of measurements and from the large kinetic differences obtained in the past work¹⁻⁵ one cannot generalize or estimate the overvoltage or the kinetics at the Al electrode in the molten alkali halides. For example one study⁴ predicts approximately 280 mV charge-transfer overvoltage at an Al anode operating at 40 mA/cm² in 50 mole % AlCl₃-50 mole % NaCl at 453 °K. At the same current density and temperature, a second study⁵ predict only 57 mV charge-transfer overvoltage in 52.8 mole % AlCl₃-47.2 mole % NaCl.

Table 1. Kinetic factors determined for aluminum in various molten halide systems.

Electrolyte composition, (mole percent)	T(°K)	Exchange current (mA/cm ²)		Tafel slope		Reference
		anodic	cathodic	Anodic (b _a)	Cathodic (b _c)	
50 AlCl ₃ -50(LiCl-KCl) _{eut}	475	1.95		$\frac{2.303 RT}{0.30 F}$		(4)
67 AlCl ₃ -33(LiCl-KCl) _{eut}	460	1.92	9.6	$\frac{2.303 RT}{0.48 F}$	$\frac{2.303 RT}{0.40 F}$	(4)
50 AlCl ₃ -50 NaCl	448	1.3	0.9	$\frac{2.30 RT}{0.28 F}$	$\frac{2.303 RT}{1.0 F}$	(4)
52.8 AlCl ₃ -47.2 NaCl	453	150	150	$\frac{2.303 RT}{1.66 F}$	$\frac{2.303 RT}{1.34 F}$	(5)
52.4 AlCl ₃ -47.6 LiCl	453	82	82	$\frac{2.303 RT}{1.62 F}$	$\frac{2.30 RT}{1.38 F}$	(5)
51.5 AlCl ₃ -48.5 KCl	453	75*	75*	$\frac{2.303 RT}{1.6 F}$	$\frac{2.303 RT}{1.4 F}$	(5)

* i^0 values extrapolated from i^0 at 720 °K using measured activation energy.

In the present work the overvoltage components and electrode kinetics of the Al electrode in 60 mole % AlCl_3 —40 mole % NaCl were studied. The present study was planned to resolve the large difference noted among past results¹⁻⁵ and to determine whether these differences could be explained by the small differences in melt composition and/or by concentration polarization at electrodes under steady current flow. For this purpose steady-state polarization curves were obtained under various conditions. Also coulomb cell data were collected to determine the number of electrons involved when an aluminum ion is discharged or dissolved in the present electrolyte.

Experimental

A more detailed description of the experimental setup and apparatus can be found in reference(6) than is presented here. The cell consisted of a one-compartment, pyrex cylinder. For kinetic measurements three aluminum electrodes were suspended from sealed joints in the top of the gas-tight cell, the test electrode lying on the axis of the cell and the other two electrodes being positioned on opposite sides of this axis. Each electrode consisted of 99.999 % pure polycrystalline Al rod with a Teflon sleeve shrunk fit over it so that only the cross sectional end was exposed to the solution. The diameter of the test electrode was 0.50 inch and the diameters of the reference and counter electrodes were 0.25 inches. The reference electrode was enclosed in a Pyrex tube which was joined to a Luggin tube and capillary. The tip of the capillary was positioned at the center of and 0.5 ± 0.2 mm away from the surface of the test electrode. Reagent grade anhydrous AlCl_3 and NaCl were melted together under a N_2 atmosphere to form the electrolyte in most of the tests. In some tests the electrolyte was made from high purity

Al and Cl_2 . High purity Al wire was added to the cell to clarify the melt. Due to sublimation of AlCl_3 from the electrolyte, it was necessary to add freshly sublimed AlCl_3 to the melt periodically. The composition of the melt was checked before and after such additions by means of EDTA titrations of the contained aluminum. The electrolyte was maintained at 453 °K by immersing the cell in a molten KNO_3 — NaNO_3 — NaNO_2 bath. Tests were made with the electrolyte both stirred and unstirred. In the former case a Teflon-coated magnetic stirring bar was used to agitate the melt.

Current *vs.* overvoltage curves were generated with an Anatrol potentiostat operated galvanostatically. For the coulometric studies the current was determined by accurately measuring the potential drop across a precision resistor.

Results and Discussion

The coulometric tests indicated that Al is both deposited and dissolved with a transfer of 3 electrons per atom. Previous work⁴ yielded the same result for electrodisolution but in that work less deposition than 1 atom was measured for the passage of 3 electrons, apparently because the deposit was so friable that some of it was lost in the transfer of the deposited Al. Through special care and handling in the present work, the weight of the deposited Al was within 4 % of the calculated weight based on the passage of charge.

Fig. 1 shows a typical anodic Tafel plot of the raw data for a freshly machined Al surface (dotted line) and for a surface on which a cathodic Tafel curve had first been run (dashed line). At each current approximately 5 min was allowed to ensure that potential drift had stopped. The stirring rate had no effect on these curves from which we rule out diffusion as the rate-determining step in anodic dissolution. No

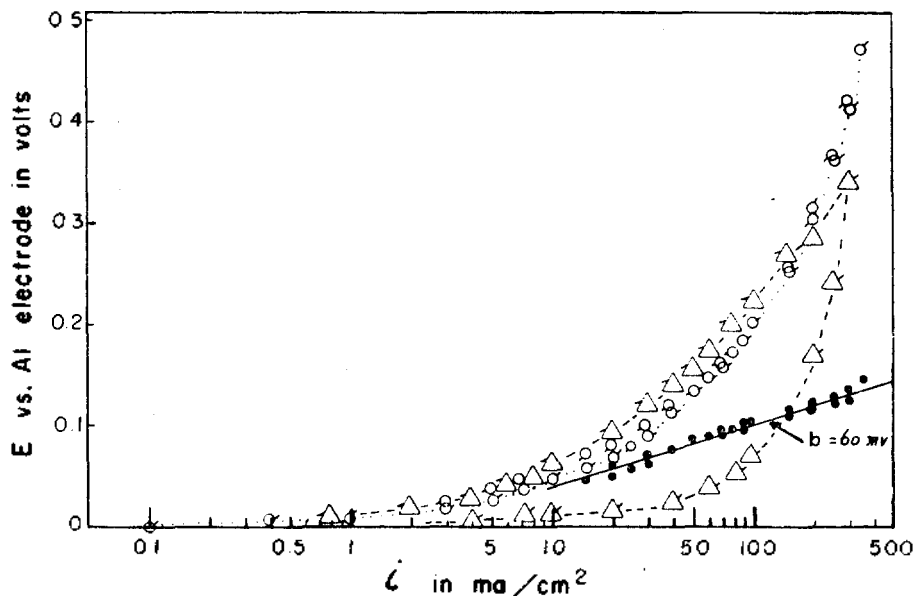


Fig. 1. Galvanostatic steady-state anodic potential (E) vs. log current curves of Al in stirred 60 mole % AlCl_3 -40 mole % NaCl ; i based on geometrical cross sectional area. \circ =fresh Al surface, raw data; \triangle =Al surface previously cathodized, raw data; \bullet =fresh Al surface, corrected for solution IR ($\rho l=0.95 \text{ ohm cm}^2$ where ρ =melt resistivity, l =distance from Al surface to Luggin capillary). Direction of flag indicates direction of current cycle (i. e., increasing or decreasing current).

hysteresis is observed in the curve for the freshly machined electrode and therefore it may be concluded that the initially smooth surface does not change appreciably during the polarization tests. For the curve following cathodic treatment of the surface the "up" curve (that at increasing current densities) is at higher current than the "down" curve. This is due to dendrites which are formed on the surface at the high currents during the cathodic cycle, and is therefore just a surface area effect. These dendrites are preferentially dissolved at the highest anodic current such that the down curve shows no effects of them. The typical cathodic polarization curve (see Fig. 2) shows a limiting current region above which there is only a slight increase in voltage with current. The curve shows hysteresis with the decreasing current cycle having the greater current. This is also due to

dendrite growth at the highest current densities. Further manifestation of this phenomena is given by the difference of appearance of the electrode before and after cathodic polarization and by the failure of the cathodic potential to increase with an increase in current at the extreme potentials; it is at these potentials past the limiting current that dendrite growth is especially rapid. Stirring of the electrolyte increased the limiting current.

In assessing the kinetics of anodic dissolution one notes that the Tafel line of Fig. 1 is curved in a manner which indicates the presence of a substantial ohmic potential drop in the electrolyte. A plot of i vs. E (see Fig. 3) is almost linear at $i > 100 \text{ mA/cm}^2$ which indicates that most of the polarization at $i > 100 \text{ mA/cm}^2$ is due to IR drop. The curve through the highest

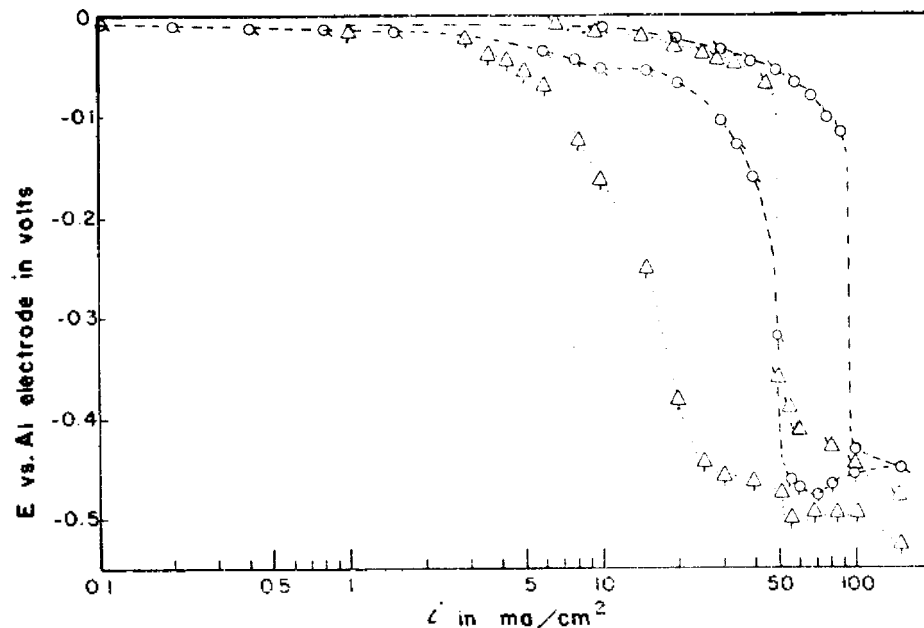


Fig. 2. Galvanostatic steady-state cathodic potential (E) vs. log current curves of Al in 60 mole % AlCl_3 -40 mole % NaCl ; i based on geometrical cross sectional area. \circ =fresh Al surface in stirred solution. \triangle =fresh Al surface in nonstirred solution.

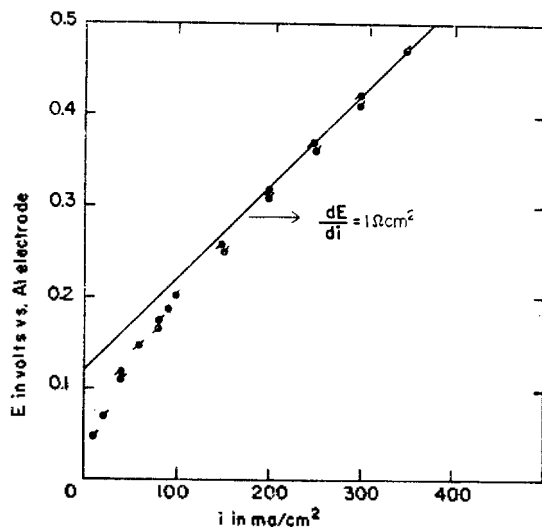


Fig. 3. Linear potential-current density plot of raw data in Fig. 1 for freshly-machined Al surface.

current values yields a value of $\frac{dE}{di} \approx 1$ ohm cm^2 (the value varied by a small amount from

one run to another as did the distance between the Luggin capillary tip and the electrode surface). When this IR drop was subtracted from the experimental Tafel curve, an essentially linear Tafel line resulted. As there is no reason to expect all the polarization to be IR drop, a more precise value of $\frac{dE}{di}$ was obtained by subtracting various IR from the raw E data until a linear Tafel plot resulted (cf. the solid circles and solid line in Fig. 1). When the value of $\frac{dE}{di}$ was too large, the corrected curve was concave downward (toward the log i axis), and when the $\frac{dE}{di}$ value was too small, the corrected curve was concave to the E axis.

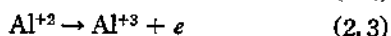
As a check on the above data treatment method, the value of the melt resistance was independently estimated. The resistivity of 60 mole % AlCl_3 -40 mole % NaCl at 180

°C (453 °K) has been determined to be 4.3 ohm cm.⁷ From this value and the electrode-Luggin separation l of 0.3 to 0.7 mm we calculate

$$\frac{dE}{di} = \rho l = 0.13 \text{ to } 0.31 \text{ ohm cm}^2. \quad (1)$$

This range of values is considerably smaller than the value (0.6 to 2 ohm cm²) obtained by linearizing the experimental Tafel plots in the present work. We believe this difference is due to the high flux of Al³⁺ into the melt at the anode which causes depletion of the Na⁺ ions at the electrode surface. As a result a layer of AlCl₃ forms, and because AlCl₃ (or an AlCl₃-rich melt of AlCl₃-NaCl) has a very low conductivity^{8,9} even the thin layer between the electrode and Luggin tip could readily result in resistivities of the magnitude necessary to explain the present results.

From the existence of well-defined, reproducible Tafel lines, we analyse the present data by considering consecutive charge-transfer steps as was done by previous investigators⁴⁻⁵. The following consecutive steps are considered;



The sum of these leads to the overall reaction



For any rate-determining step and with the other

steps in quasi-equilibrium an expression may be derived for the overall rate and apparent transfer coefficients in terms of the rate constants and charge-transfer coefficients for the individual steps,

$$i = i^0 (\exp(\alpha_a F \eta / RT) - \exp(-\alpha_c F \eta / RT)) \quad (4)$$

where i and η are positive for anodic and negative for cathodic current and where α_a and α_c are the apparent anodic and cathodic transfer coefficients, respectively of reaction(3). For each step in (2) being rate determining, α_a and α_c are listed in terms of the constituent steps in Table 2.

All of the anodic Tafel "b" values ($b = dE/d \log i$) for the 7 curves developed lie between 50 and 70 mV and yield an overall average of 60 mV. This corresponds to the apparent anodic transfer coefficient, α_a (cf. Eq.(4)) of 1.5 ± 0.25 and $i_0 \approx 3 \text{ mA/cm}^2$. Allen-Hickling plots constructed from the IR-corrected polarization data yielded results which are typified in Fig. 4. The corresponding slopes are interpreted from Eq. 4 and from the fact that $\alpha_c = 3 - \alpha_a$ (cf. Table.2 and the explicit derivations in references (4) and (5)); i. e.

$$\frac{i}{1 - \exp(-3F\eta/RT)} = i_0 \exp(\alpha_a F \eta / RT) \quad (5)$$

The Allen-Hickling plot yields an apparent

Table. 2 Calculated apparent transfer coefficients, α_a and α_c , for various steps in (2) being rate-determining.

Rate-determining step	(α_a) Anodic transfer coefficient	(α_c) Cathodic transfer coefficient
2.1	$\alpha_{2.1}$	$3 - \alpha_{2.1}$
2.2	$1 + \alpha_{2.2}$	$2 - \alpha_{2.2}$
2.3	$2 + \alpha_{2.3}$	$1 - \alpha_{2.3}$
experimental: 60 mole % AlCl ₃ -40 mole % NaCl at 453°K	$1.5 \pm .25$ ($\eta > 0$)	1.7 ($0 > \eta > -40 \text{ mV}$) 2.6 ($\eta < -40 \text{ mV}$)

* $\alpha_{2.1}$, $\alpha_{2.2}$, $\alpha_{2.3}$ represent the charge-transfer coefficients for steps (2.1), (2.2) and (2.3) respectively and $0 < \alpha_{2.1} < 1$

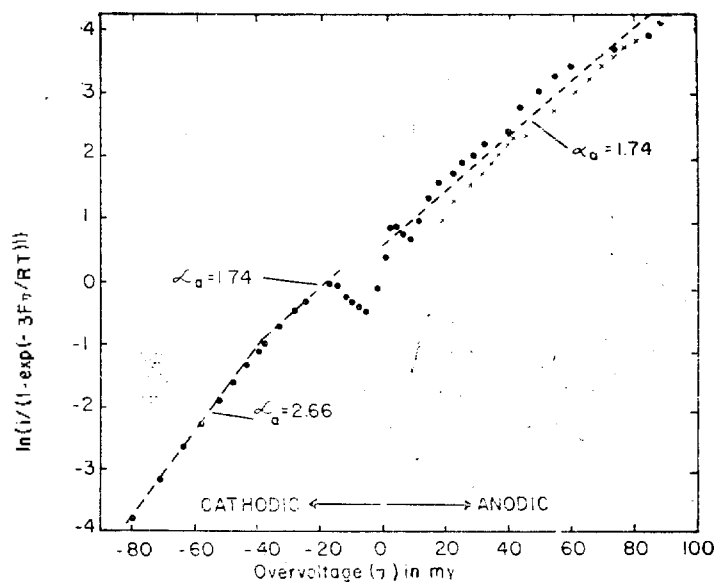


Fig. 4. Allen-Hickling plot of IR-corrected anodic and cathodic steady-state polarization data on fresh Al surface in 60 mole % AlCl_3 -40 mole % NaCl. Electrolyte stirred. ●=increasing current cycle; ×=decreasing current cycle; curves obtained galvanostatically

anodic transfer coefficient which is equivalent to that obtained from the Tafel plot. For cathodic overvoltages between 20 and 40 mV the Allen-Hickling plot yields a straight line with a slope corresponding to $\alpha_a=1.74$ ($\alpha_c=1.26$). At $\eta=-40$ mV the slope changes to yield $\alpha_a=2.66$ ($\alpha_c=0.34$); dendrite growth prevented measurements at higher overvoltages. At $0 > \eta > -20$ mV the data points do not fall on the well-defined Allen-Hickling lines. This is due to the effects of trace amounts of oxygen or water in the melt which are negligible in their influence except near zero current. A black film slowly formed under these conditions which microprobe analysis proved to contain aluminum and oxygen; scanning electron microscopy revealed crystals which had the appearance of aluminum oxide⁶. These trace amounts of oxygen or water were too minute to interfere with the polarization curves except at near zero current as noted above. At higher current densities or

with the anodic tests in which the surface is continually renewed they are without effect. For the present system the anodic charge-transfer coefficient is 1.5 ± 0.25 for $i=0$ to 300 mA/cm^2 ; correspondingly only step(2b) can be rate-determining in accordance with the limitation that $\alpha_{2,x}$ be between 0 and 1. The cathodic Allen-Hickling slope indicates that (2b) is the rate-determining step for $\eta > -40$ mV and that (2a) is the rate-determining step for $\eta < -40$ mV.

The presently obtained transfer coefficient and mechanism for Al dissolution and deposition in 60 mole % AlCl_3 -40 mole % NaCl agree with those developed by Schulze and Hoff⁵ for Al in 52 mole

% AlCl_3 -48 mole % HCl. It therefore appears that small changes in melt composition (e.g. from 60 mole percent AlCl_3 to 51.5 mole percent AlCl_3) do not change the reaction mechanism. The present results also agree with battery studies¹⁻³ in predicting substantial ohmic potential losses at high current densities. At practical-electrode separations expected in batteries, the melt resistance would contribute appreciably to the anodic polarization. In addition concentrating the anolyte with aluminum ions would add another large polarization independent of the electrode separation.

Acknowledgement

The authors wish to thank the National Institutes of Health, Grant GP 12862, National Science Foundation, Grant GP 28631, and the Army Research-Durham, Contract DA-ARO-

D-31-124172-G15, for support of this work.

References

1. R. Piontelli, G. Sternheim and M. Francini, *J. Chem. Phys.*, **24**, 1113(1956).
2. L. A. King, A. D. Brown, Jr. and F. H. Frayer, Proc. OAR Research Applications Conference, Vol. 1, Rep. OAR-68-001. Institute for Defense Analyses, 1968.
3. G. D. Brabson, Jr., A. A. Fannin Jr., L. A. King and D. W. Seegmiller, USAF Report No. SRL-TR-72-0013, Frank J. Seiler Research Laboratory(AFSC), USAF Academy, Colorado, 1972.
4. B. S. Del Duca, Nasa Report No. TND-5503, Lewis Research Center National Aeronautics and Space Administration, Cleveland, 1969.
5. K. Schulze and H. Hoff, *Electrochim. Acta*, **17**, 119(1972).
6. G. F. Uhlig, Ph. D. thesis, University of Utah, Salt Lake City, Utah, 1973.
7. C. R. Boston, L. F. Grantham and S. J. Yosim, *J. Electrochem Soc.*, **117**, 28(1970).
8. R. H. Moss, Ph. D. Thesis, University of Connecticut, 1955.
9. C. R. Boston, S. J. Yosim, and L. F. Grantham, *J. Chem. Phys.*, **51**, 1669(1969).